Parametric study of dynamic supporting force of WIG marine vehicles

Mohamed A. Kotb and Yasser M. Ahmed
Marine Eng. and Naval Architecture Dept., Faculty of Eng., Alexandria University, Alexandria, Egypt

The past decade has witnessed a rapid growth of interest in the development of fast and advanced marine vehicles for various applications. In this study the Wing In Ground effect crafts (WIG crafts) have been introduced as an example of high speed advanced marine vehicles that represent a new era in the waterborne transportation. The WIG crafts work near water or ground surfaces and the benefit of operation in ground proximity is manifested in higher lift and lower drag. A simple analysis based on single element lumped vortex or horseshoe vortex element for infinite and finite lifting plate, respectively, was used to examine the effect of ground proximity on dynamic supporting force or lift characteristics. Two parameters were identified; the first is inclusive of wing geometry represented by aspect ratio while the other parameter includes the cruising altitude ratio. A plot was suggested to determine an apparent aspect ratio accounting for the gain resulting from the ground proximity.

شهد العقد المنصرم اهتماما متزايدا بتطوير المركبات البحرية السريعة ومن أحدث هده المركبات ظهر ما يعرف بمركبة الويج، وهذا المركبة البحرية تعمل في الهواء قريبا من سطح الماء حيث تكون قوة الرفع الديناميكية المتولدة بواسطة أجنحة خاصة كبيرة وذلك كلما زاد اقتراب المركبة من سطح الماء. في هذا البحث تم دراسة قوة الرفع الديناميكية باستخدام نظرية خط الرفع في كل من حالتي الجناح ثنائي الأبعاد و ثلاثي الأبعاد (محدد البحر). تم تعريف معاملين (بارا مترين) أحدهما خاص بأبعاد سطح الرفع والأخر يتعلق بالارتفاع الذي تحلق فيه المركبة وعلاقة هذين المعاملين بقوة الرفع الديناميكية المتولدة وتأثير الاقتراب من سطح الأرض أو الماء علي هذه القوة.

Keywords: WIG craft, Ground effect, Dynamic lift, Effective aspect ratio, Advanced marine vehicles

1. Introduction

Marine vehicles may be classified according to different criteria such as navigational route, working area with respect to the water surface, material of construction, mission, lifting force... etc.

Based on the type of lifting force required to vertically support the craft, marine vehicles are grouped as shown in fig. 1.

The most recent member which has joined marine vehicles family is Wing In Ground effect vehicle, or WIG.

A Wing In Ground (WIG) effect vehicle is a craft that is especially designed to take advantage of the reduced drag and increased lift of ground effect. Therefore a WIG vehicle will always fly close to the surface. Although it is called *ground* effect, most WIG vehicles only fly over water, but some are amphibious.

The main difference between a WIG and air cushion vehicles ACV's or surface effect ship SES's is that a WIG vehicle rides on a *dynamic* air cushion as opposed to a hovercraft, which rides on a *static* air cushion. The WIG generates lift by forward speed, but the hovercraft has fans that continuously blow up the cushion. This is why a WIG is much more (fuel) efficient than a hovercraft.

During the last decades a large number of very different WIG vehicles have been designed and built [1]. Most of these designs were built for military purposes. Commercial production already started in the USA. [2] and Australia [3].

WIG vehicles can be classified into four different configurations: Ram Wing, Lippisch, Tandem, and Ekranoplan; fig. 2. In 1995, the International Maritime Organization (IMO) recognized and issued regulations concerning wing in ground effect vehicles [4].

In this paper, the effect of ground proximity on the supporting lift was parametrically studied. Simple explanations were given.

Alexandria Engineering Journal, Vol. 41 (2002), No. 5, 793-800

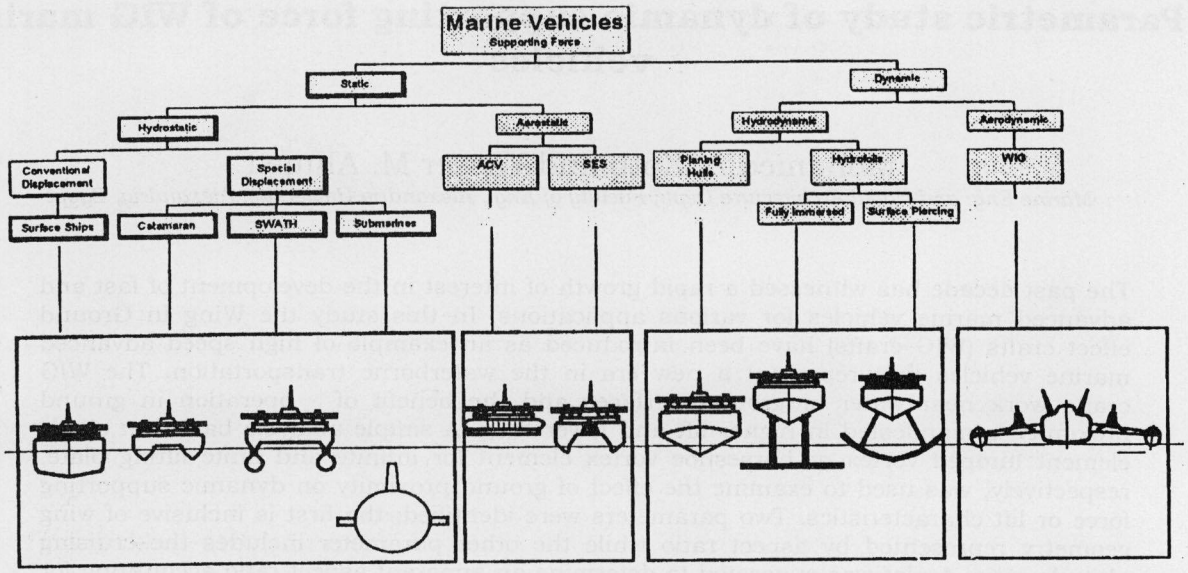

Fig. 1. Marine vehicles according to supporting force,

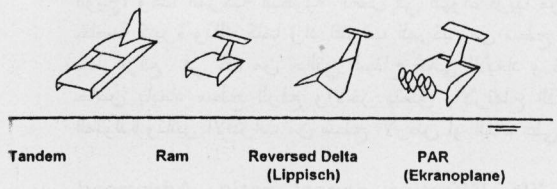

Fig. 2. WIG vehicles types.

The effects of main geometrical particulars are studied. Formula for apparent or effective aspect ratio based on lift characteristics was derived.

2. Parametric study

The wing platform is replaced by a bound vortex (lifting line) along its span and located at the quarter chord position. Two trailing (free) vortices extending to infinity in the downstream directions are used to account for the wing tips. The system comprised of the three equal strength vortices is termed horseshoe system. Application of the boundary condition; that the flow is tangent to the wing surface (i.e., there is no flow through the surface) is used at a control point centered spanwise on the three-quarter-chord line midway between the two trailing vortex legs.

The influence of ground or water surface proximity on the wing performance can be investigated by the method of images where the ground is simulated by an image distanced down below the actual wing; fig. 3.

3. Lift generated by an infinite wing (2D) in the presence of the ground

Fig. 4 shows the equivalent system for a wing in ground effect. The boundary condition of zero normal velocity is applied at a control point at three quarter chord length; on the actual wing. Therefore,

$$V_\infty \sin\alpha - \frac{\Gamma}{2\pi l} + \frac{\Gamma}{2\pi l_1} = 0 . \qquad (1)$$

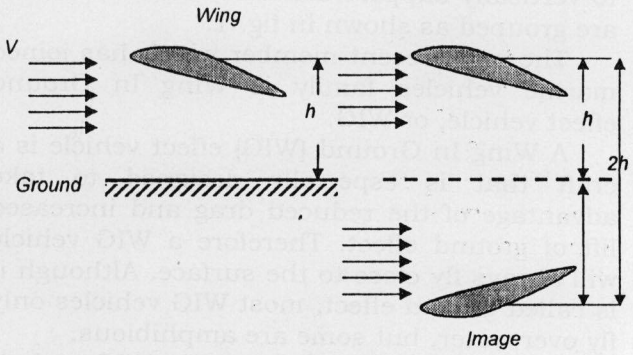

Fig. 3. Wing in ground effect and its equivalent system.

Where, distances l and l_1 are shown on fig. 4. Solving eq. (1) for the required circulation Γ_{IGE} in case of ground effect,

$$\Gamma_{IGE} = 2\pi V_\infty \sin\alpha \frac{l l_1}{(l_1 - l\cos\varphi)}. \quad (2)$$

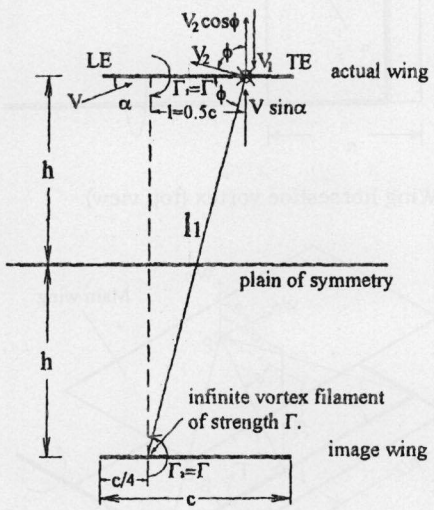

Fig. 4. Equivalent system for a wing in ground effect.

Meanwhile, the circulation in Off Ground condition (OGE) is:

$$\Gamma_{OGE} = 2\pi V_\infty l \sin\alpha. \quad (3)$$

The ratio of the circulation values in and out of ground after geometrical substitution is:

$$\frac{\Gamma_{IGE}}{\Gamma_{OGE}} = 1 + \frac{c^2}{16h^2},$$

and the ratio of circulation increase due to ground proximity is:

$$\frac{(\Gamma_{IGE} - \Gamma_{OGE})}{\Gamma_{OGE}} = \frac{\Delta\Gamma}{\Gamma_{OGE}} = \frac{1}{16(h/c)^2}. \quad (4)$$

Hence, the lift force, L, per unit length can be calculated from Kutta-Joukowski relation ref. [5] $L = \rho_\infty V_\infty \Gamma$ as:

$$L = \frac{(2\pi\rho_\infty V_\infty^2 \sin\alpha) l l_1}{(l_1 - l\cos\varphi)}. \quad (5)$$

From the geometry of fig. 4, eq. (5) can be written as:

$$L = \pi\rho_\infty V_\infty^2 c \sin\alpha \left(1 + \frac{c^2}{16h^2}\right). \quad (6)$$

Hence, the lift coefficient C_L will be,

$$C_L = \frac{L}{0.5\rho V_\infty^2 c} = 2\pi \sin\alpha \left(1 + \left(\frac{c}{4h}\right)^2\right). \quad (7)$$

In eq. (7) when $h \to \infty$, the lift coefficient, $(C_{L_{h\infty}})$, far away from the ground will be,

$$C_{L_{h\infty}} = 2\pi \sin\alpha. \quad (8)$$

From eqs. (7) and (8) we can get lift coefficient, C_{Lh}, at any height h in terms of its out of ground (OGE) counterpart as:

$$C_{L_h} = C_{L_{h\infty}} \left(1 + \left(\frac{c}{4h}\right)^2\right), \quad (9)$$

and the increase in lift due to ground proximity is:

$$\frac{(C_{Lh} - C_{L\infty})}{C_{L\infty}} = \frac{\Delta C_L}{C_{L\infty}} = \frac{1}{16(h/c)^2}, \quad (10)$$

which is identical to eq. (4).

Both eqs. (4) and (10) are displayed in fig. 5. The graph shows that the effect of getting close to the ground is neglected for $h/c > 0.8$, where the lift increases will be less than 10 percent. The results arrived at in eqs. (4) and (9) are similar to those obtained in Katz [6] for thin airfoils using perturbation expansion. The lift coefficient obtained was as:

$$C_L = 2\pi\alpha \left[1 + \frac{1}{4}\left(\frac{h}{2c}\right)^{-2} + O\left(\frac{h}{2c}\right)^{-4}\right].$$

4. Lift generated by a finite wing in the presence of the ground

For a rectangular wing of finite span, tips are represented by two free (trailing) vortices of strength Γ in addition to the wing bound

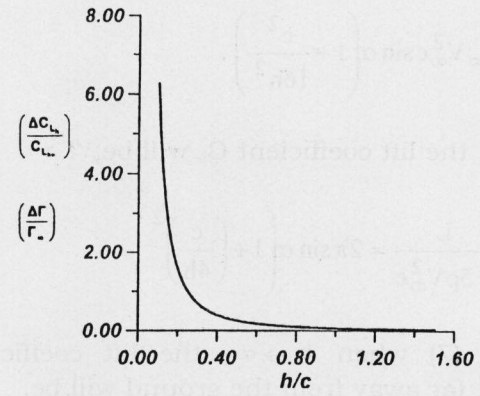

Fig. 5. 2D lift and circulation increase ratio of a flat plate with height ratio from the ground at 5° incidence.

vortex. An image horseshoe vortex of strength $-\Gamma$ lies beneath the actual wing by a distance 2h from its leading edge.

Using Biot-Savart law, ref. [5] the downwash velocity v_P at any point P, induced by a vortex segment is obtained in terms of distance h and angles α and β as:

$$v_p = \frac{\Gamma}{4\pi h}(\cos\alpha + \cos\beta). \qquad (11)$$

For the vortex system shown on fig. 6, where w_1 is the component induced by the bound vortex, w_2 and w_3 are components induced by the right and left trailing vortices, respectively

Hence, for a wing control point P:

$$w_1 = \frac{\Gamma}{\pi c}\left[\frac{b}{\sqrt{b^2+c^2}}\right], \qquad (12)$$

$$w_2 = w_3 = \frac{\Gamma}{2\pi b}\left(\frac{c}{\sqrt{b^2+c^2}}+1\right). \qquad (13)$$

Hence, the total induced velocity at point P is,

$$w = \sum_{i=1}^{3} w_i = \frac{\Gamma}{\pi bc\sqrt{b^2+c^2}}\left[b^2 + c\left(c+\sqrt{b^2+c^2}\right)\right]. \qquad (14)$$

Similarly, the normal component (to the wing) of the velocity induced by the image bound vortex at the control point will be as shown in fig. 7.

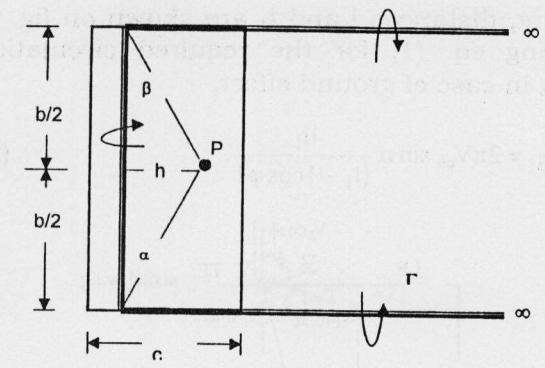

Fig. 6. Wing horseshoe vortex (top view).

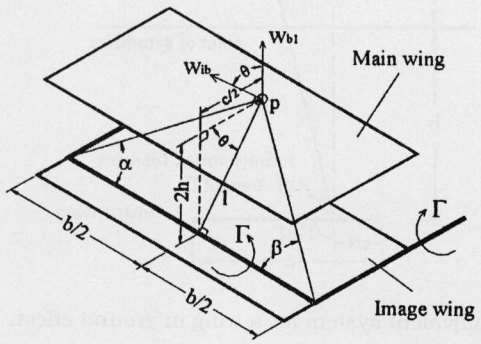

Fig. 7. The image bound vortex.

$$w_{bl} = \left(\frac{\Gamma}{\pi}\right)\left(\frac{c}{16h^2+c^2}\right)\left(\frac{b}{\sqrt{16h^2+c^2+b^2}}\right). \qquad (15)$$

Similarly the contribution from the trailing vortices of the image wing at the control point normal to the wing is:

$$w_{tl} = 2\left[\frac{\Gamma}{2\pi}\left(\frac{b}{16h^2+b^2}\right)\left(\frac{c}{\sqrt{16h^2+c^2+b^2}}+1\right)\right]. \qquad (16)$$

The total normal induced velocity, w_i, generated by the image wing at the control point P will be: $w_i = w_{bl} + w_{tl}$, hence:

$$w_i = \left(\frac{\Gamma}{\pi}\right)\left(\frac{b}{\sqrt{16h^2+c^2+b^2}}\right)\times \left[\left(\frac{c}{16h^2+c^2}\right)+\left(\frac{1}{16h^2+b^2}\right)\left(c+\sqrt{16h^2+c^2+b^2}\right)\right]. \qquad (17)$$

The boundary condition of zero normal velocity at the control point P will be,

$$V_\infty \sin\alpha - w_i + w = 0 . \quad (18)$$

Substituting eqs. (14) and (17) into eq. (18) and solving for Γ we get:

$$\Gamma = \frac{V_\infty \sin\alpha}{H_1 - H_2} . \quad (19)$$

Where,

$$H_1 = \left[\frac{1}{\pi bc\sqrt{b^2+c^2}}\left[b^2 + c\left(c+\sqrt{b^2+c^2}\right)\right]\right], \quad (20)$$

$$H_2 = \left(\frac{1}{\pi}\right)\left(\frac{b}{\sqrt{16h^2+c^2+b^2}}\right) \left[\left(\frac{c}{16h^2+c^2}\right)+ \left(\frac{1}{16h^2+b^2}\right)\left(c+\sqrt{16h^2+c^2+b^2}\right)\right]. \quad (21)$$

If we substitute $AR = \frac{b}{c}$ for rectangular wing where AR is the wing aspect ratio, H_1, and H_2 can be written as:

$$H_1 = \frac{\sqrt{1+AR^2}+1}{\pi b}, \quad (22)$$

$$H_2 = \frac{AR^2}{b\pi\sqrt{16(h/c)^2+1+AR^2}} \times \left[\left(\frac{1}{16(h/c)^2+1}\right)+ \left(\frac{1+\sqrt{16(h/c)^2+AR^2+1}}{16(h/c)^2+AR^2}\right)\right]. \quad (23)$$

The lift force, L, per unit length produced by the finite wing of rectangular platform in ground effect can be calculated from:

$$L = \rho_\infty V_\infty \left(\frac{V_\infty \sin\alpha}{H_1 - H_2}\right), \quad (24)$$

and the corresponding lift coefficient, C_L, in this case will be,

$$C_L = \frac{L}{0.5\rho V_\infty^2 c} = \left(\frac{2AR}{b}\right)\left(\frac{\sin\alpha}{H_1 - H_2}\right). \quad (25)$$

Fig. 9 represents the relation between the height ratio, h/c, and the lift coefficient, C_L, as given by eq. (25), for different aspect ratios, at 5^0 angle of incidence.

It is worth noting that the term H_1 given by eq. (22) is only related to wing geometry or in other words wing aspect ratio AR, while the term H_2 is a function of both AR and wing elevation from the ground; that is (h/c) term. As the ratio h/c tends to infinity; (wing is operating in off ground conditions), the term H_2 tends to zero, and we are left with only the term H_1 in eq. (25).

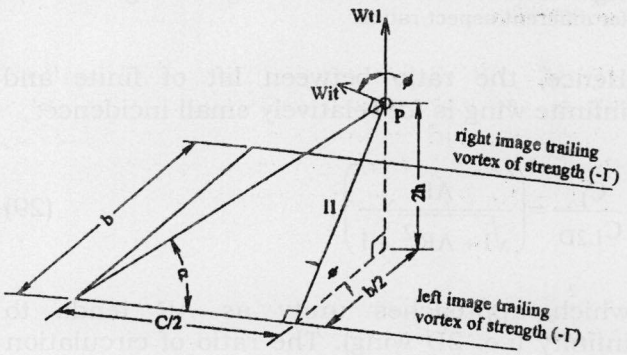

Fig. 8. The image trailing vortex.

Hence the lift coefficient in this case is:

$$C_L = \left(\frac{2AR}{b}\right)\left(\frac{\sin\alpha}{H_1}\right), \quad (26)$$

and the circulation in off ground condition (OGE) will be:

$$\Gamma_{OGE} = \frac{V_\infty \sin\alpha}{H_1} . \quad (27)$$

And substituting eq. (22) in eq. (26), we get:

$$C_L = \left(2\pi \sin\alpha \frac{AR}{\sqrt{1+AR^2}+1} \right). \quad (28)$$

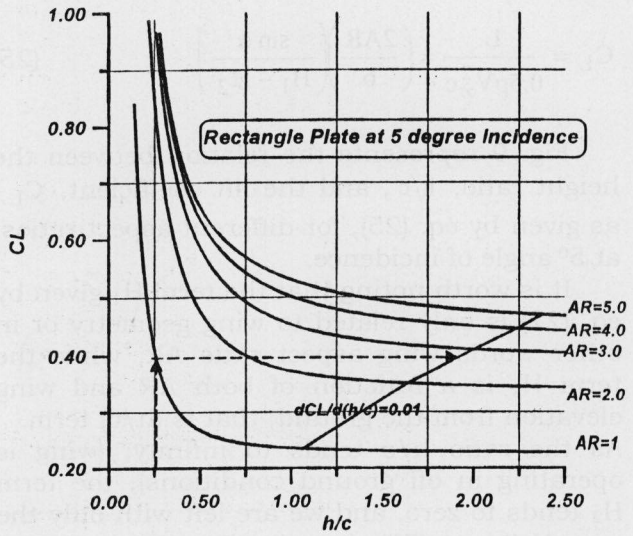

Fig. 9. Lift coefficient C_L for a rectangular wing versus h/c for different aspect ratios.

Hence, the ratio between lift of finite and infinite wing is for relatively small incidence:

$$\frac{C_L}{C_{L2D}} = \left(\frac{AR}{\sqrt{1+AR^2}+1} \right), \quad (29)$$

which approaches unity as AR tends to infinity (i.e. 2D wing). The ratio of circulation between in and off ground circulations will be,

$$\frac{\Gamma_{IGE}}{\Gamma_{OGE}} = \left(\frac{H_1}{H_1 - H_2} \right) = \frac{1}{1-(H_2/H_1)}. \quad (30)$$

From eqs. (29) and (30), we can express lift and circulation increase due to ground proximity as:

$$\frac{\Delta C_L}{C_L} = \frac{H_2}{H_1 - H_2} = f(AR, h/c, \alpha), \quad (31)$$

$$\frac{\Delta\Gamma}{\Gamma_{OGE}} = \frac{H_2}{H_1 - H_2} = f(AR, h/c, \alpha). \quad (32)$$

Eqs. (31) and (32) are plotted on fig. 12 for different H_1 value. It is shown that both lift and circulation increases as parameter H_2 increases which means either aspect ratio increases or distance above the ground decreases or both. The lift or circulation increases to infinity when the value of H_2 approaches H_1 ratio which is satisfied at h/c=0. No increase occurs when the wing is off ground or in free unbounded flow. This case is represented by the horizontal axis. It is quite interesting here to see that for the lower portion of the figure reduction in both lift and circulation is reported. This is actually corresponds to motion in submergence condition where the lifting surface is moving near the water or free surface. In such case, the height ratio is negative and lower lift is expected. This result is confirmed in Thirat [8].

An interesting condition will arise when $H_1=H_2$. This is attained when h/c=0 (limiting hypothetical condition) regardless the aspect ratio value as:

$$H_2 = \frac{AR^2}{b\pi\sqrt{1+AR^2}} \left[1 + \left(\frac{1+\sqrt{AR^2+1}}{AR^2} \right) \right],$$

$$H_2 = \frac{1}{b\pi\sqrt{1+AR^2}} \left[AR^2 + 1 + \sqrt{AR^2+1} \right], \quad (33)$$

$$H_2 = \frac{1}{b\pi} \left[1 + \sqrt{AR^2+1} \right] = H_1,$$

and in this case C_L will tend to infinity.

Fig. 11 shows the variation of parameters H_1 and H_2 as given by eqs. (22) and (23). It is clearly shown that H_1 is only a function of aspect ratio while H_2 is function of both aspect ratio and height ratio above the ground. H_1 increases as the aspect ratio increases. H_2 increases as aspect ratio increases and height ratio decreases. H_2 approaches H_1 as h/c tends to zero. H_1 also presents a ceiling value for H_2 which is reached where h/c is typically zero. In other words, H_2 is always less than H_1 for all values of aspect ratios and for all positive values of h/c.

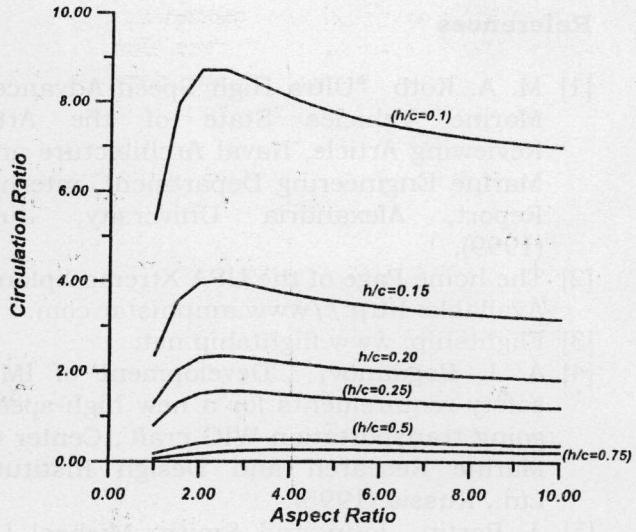

Fig. 10. Circulation ratio versus Aspect Ratio (AR).

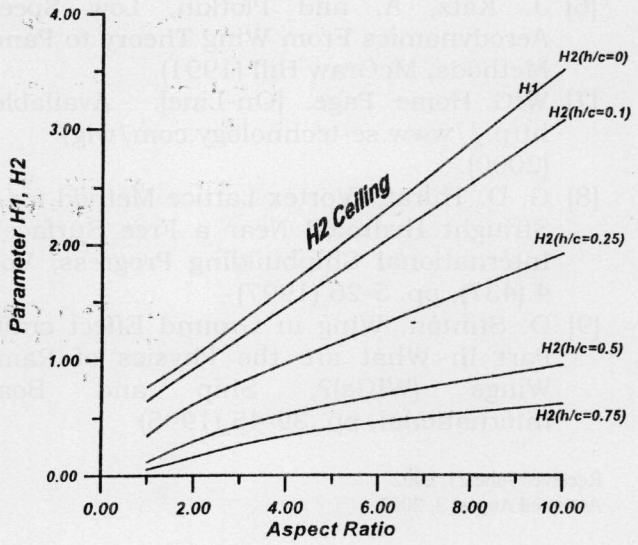

Fig. 11. Parameters H_1 and H_2 versus aspect ratio and height ratio.

5. Apparent aspect ratio

Fig. 9 could be used to estimate the wing "effective" aspect ratio that is the virtual or apparent geometrical aspect of the same wing when working in off ground effect mode. It is assumed here that the lift ceases to increase with decrease of height ratio h/c if its derivative with respect to height is less λ or equal to 1%. A line representing λ to this value is sketched or constructed on the same plot. The to 1% value for $dC_L/d(h/c)$ corresponds to different h/c values at different aspect ratio. For a wing of a known geometrical aspect ratio working at a known altitude, one can use the 1% line to determine the apparent or virtual aspect ratio that accounts for the ground proximity. For example a wing with geometrical aspect ratio of 1.0 at 0.26 h/c is equivalent to a 2.6 aspect ratio wing working in an unlimited flow. Physical explanation for wing-increased lift when working near the ground is qualitatively given in [7, 9].

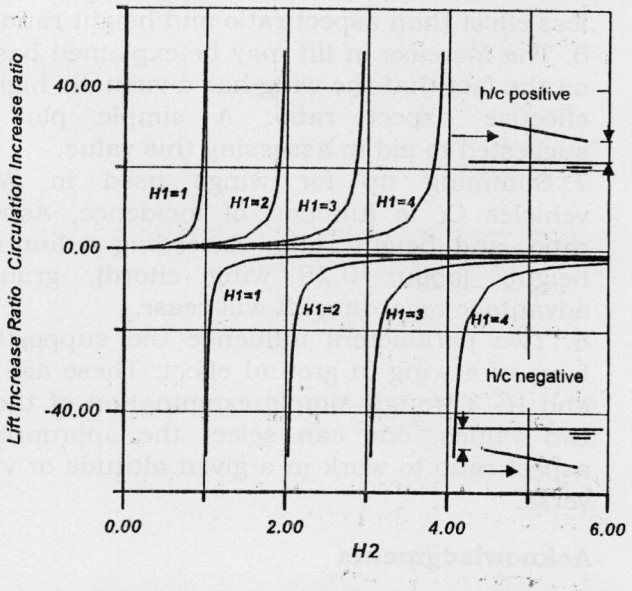

Fig. 12. Lift and circulation increase versus parameter H_2 for different H_1 values.

6. Conclusions

A number of remarks and observations are concluded from the above work.

1. For 2D plane lifting surface, the effect of operation close to the ground or water surface is more pronounced at altitudes less than quarter chord.
2. A simple parametric analysis on the influence of the ground effect phenomenon using the method of images on a rectangular wing of finite span indicated the increase of dynamic lift generated by the wing when it gets close to the ground or water surface.
3. The parametric study conducted on the performance of a wing in ground effect vehicle aimed at shedding the light on the factors affecting its performance. Some of these factors ate related to the wing geometrical

characteristics, while the others due to the operating conditions.

4. The geometric parameters such as the aspect ratio, AR , has the effect of increasing the lift forces of wings of finite platforms. This fact has been verified in this study for both in and off ground effect modes of operation.

5. It is recommended to include other factors such as camber and thickness, sweep, dihedral angles to examine their effects on wing performance, which should improve the performance predictions, even though having less effect than aspect ratio and height ratio.

6. The increase in lift may be explained based on the fact that the wing has a virtually higher effective aspect ratio. A simple plot is suggested to aid in assessing this value.

7. Summing up for wings used in WIG vehicles C_L is function of incidence, Aspect ratio, and height ratio. Exceeding a limiting height, (about 0.25 wing chord), ground advantage regarding lift will cease.

8. Two parameters influence the supporting force of a wing in ground effect. These are H_1 and H_2. Through simple examination of these two values, one can select the appropriate aspect ratio to work in a given altitude or vise versa.

Acknowledgments

The authors would like to thank professors A. S. Sabet and A. Elbadan for their valuable contributions throughout this work.

References

[1] M. A. Kotb "Ultra High Speed Advanced Marine Vehicles State of the Art", Reviewing Article, Naval Architecture and Marine Engineering Department, internal Report, Alexandria University, July (1999).

[2] The home Page of the USA Xtreme Xplorer Available: http://www.amphistar.com.

[3] Flightship; www.flightship.net.

[4] A. I. Bogdanov, 'Development of IMO safety requirements for a new high-speed going transportation-WIG craft', Center of Marine Research and Design Institute Ltd., Russia (1995).

[5] J. Bertin, John and Smith, Michael L., Aerodynamics for Engineers, Prentice Hall, Inc., Englewood Cliffs (1979).

[6] J. Katz, A. and Plotkin, Low Speed Aerodynamics From Wing Theory to Panel Methods, McGraw Hill (1991).

[7] WIG Home Page. [On-Line]. Available: http://www.se-technology.com/wig/ (2000).

[8] G. D. Thirat, "Vortex Lattice Method for a Straight Hydrofoil Near a Free Surface", International Shipbuilding Progress, Vol. 4 (437), pp. 5-26 (1997)

[9] D. Stinton, Wing in Ground Effect craft, Part II: What are the Physics of Ram-Wings (WIGs)?, Ship and Boat International, pp. 39-45 (1995)

Received June 23, 2002
Accepted August 3, 2002